Supporting Information for

Single-Crystal Structure of a Covalent Organic Framework

Yue-Biao Zhang,[†,§] Jie Su,[‡,§] Hiroyasu Furukawa,[†] Yifeng Yun,[‡] Felipe Gándara,[†] Adam Duong,[†] Xiaodong Zou,[‡,] and Omar M. Yaghi[†,*]*

[†]Department of Chemistry, University of California, and Materials Sciences Division, Lawrence Berkeley National Laboratory, Berkeley, California 94720, United States

[‡]Inorganic and Structural Chemistry and Berzelii Center EXSELENT on Porous Materials, Department of Materials and Environmental Chemistry, Stockholm University, Stockholm SE−106 91, Sweden

Table of Contents

Section S1. *General information and synthetic procedures.*

Materials: 4,4'-Biphenyldicarbaldehyde was purchased from TCI Co; tetra-(4-anilyl)-methane was synthesized according to the literature;[1] anhydrous solvents were obtained from Sigma-Aldrich Co.

Synthesis and Activation of COF-320: Biphenyl-4,4'-dicarbaldehyde (BPDA, 100 mg, 0.476 mmol) and tetra-(4-anilyl)-methane (TAM, 100 mg, 0.263 mmol) were dissolved in 5 mL of anhydrous dioxane within a Pyrex tube (o.d × i.d = 10 mm × 8 mm) under sonication. After quick freezing the solution with liquid N_2, 1 mL of aqueous acetic acid (3 mol/L; by dissolving glacier acetic acid in deionized water) was added into the tube, which was then connected to Schlenk line through a short rubber hose with stopcock. After a couple times of freeze-pump-thaw cycles, the frozen tube was vacuumed to 50 mTorr and insulated by close the stopcock. The tube was then quickly sealed with a torch reducing the length of the tube into 18-20 cm. After heating at 120 ºC for 72 h, yellow solid at the bottom of the tube was isolated by hot filtration and washed with anhydrous tetrahydrofuran (THF). The obtained powder was immersed in anhydrous THF, and the solvent was exchanged with fresh THF for several times and anhydrous acetone for one time. The wet sample was then transfer to a super critical drier, in which the sample was washed with five times of liquid CO_2, and exchanged with fresh CO_2 for 5 times with the interval of half hour. The system was heat up to 45 ºC to bring about the supercritical state of the CO_2, which was bleed after half hour in very slow flow rate to ambient pressure. The sample was then transferred to vacuum chamber and evacuated to 20 mTorr under room temperature, yielding bright-yellow powder 120 mg (ca. 70% yield based on the BPDA). Elemental analysis: Calcd. for $C_{53}H_{36}N_4$: C, 87.33; H, 4.98; N, 7.69%. Found: C, 86.99; H, 4.91; N, 7.51%.

Synthesis of the molecular analogue of COF-320, (*NE*,*N'E*,*N''E*,*N'''E*)-4,4',4'',4'''-methanetetrayltetrakis(*N*-([1,1'-biphenyl]-4-ylmethylene)aniline).

A mixture of tetra-(4-anilyl)methane (100 mg, 0.263 mmol) and biphenyl-4-carbaldehyde (250 mg, 1.373 mmol) in anhydrous *p*-xylene (25 mL) was stirred under reflux with a Dean-Stark apparatus over 24 hours. An off-white solid was precipitated out after cooling down the mixture to room temperature, which was collected by filtration and dried under vacuum (270 mg, 99% yield). ^{1}H NMR (600 MHz, $CDCl_3$) ä 8.6 (s, 4H), 7.99 (d, 8H, ^{3}J = 7.6 Hz), 7.72 (d, 8H, ^{3}J = 8.1 Hz), 7.65 (d, 8H, ^{3}J = 7.6 Hz), 7.47 (t, 8H, ^{3}J = 7.6 Hz), 7.39 (t, 4H, ^{3}J = 7.3 Hz), 7.33 (d, 8H, ^{3}J = 8.5 Hz), 7.21 (d, 8H, ^{3}J = 8.1 Hz). ESI MS for $C_{77}H_{56}N_4$ (Calcd. 1036.45): *m*/*z* =1037.4612 ($[M+1]^+$, 100%); Elemental analysis: Calcd. for $C_{77}H_{56}N_4$: C, 89.16; H, 5.44; N, 5.40%. Found: C, 88.90; H, 5.31; N, 5.30%.

X-ray single-crystal structure analysis of E: Single-crystals of the molecular analogue of COF-320 (**E**) were crystallized by the slow diffusion of hexane vapor into a solution of CH_2Cl_2 containing **E**. A colorless blocks crystal (0.12 × 0.14 × 0.25 mm) was mounted on a Bruker D8 Venture diffractometer equipped with a fine-focus Cu target X-ray tube operated at 40 W power (40 kV, 1 mA) and a PHOTON 100 CMOS detector. The specimen was cooled to -123 °C using an Oxford Cryosystem chilled by liquid nitrogen. Bruker APEX2 software package was used for data collection; SAINT software package was used for data reduction; SADABS was used for absorption correction; no correction was made for extinction or decay. The structure was solved by direct methods in a tetragonal space group $I4_1/a$ with the SHELXTL software package and further refined with least squares method. All non-hydrogen atoms were refined anisotropically, all hydrogen were generated geometrically. The details of crystallography data are shown in Table S1.

Table S1. Crystal data and structure refinement for molecular analogue **E**.

Chemical Formula	$C_{77}H_{56}N_4 \cdot CH_2Cl_2$
Formula weight	1122.18
Crystal system	Tetragonal
Space group	$I4_1/a$ (No. 88)
a/Å	28.713(2)
c/Å	7.4609(4)
V/Å^3	6151.0(6)
Z	4
d_{calc} /g cm^{-3}	1.212
Radiation	Cu Kα
Wavelength/Å	1.54178
Temperature/K	150
Crystal size/mm^3	0.12 × 0.14 × 0.25
Crystal color	yellow
Theta Min-Max/°	3.1, 61.7
Tot./Uniq. Data	18875/2344
R_{int}	0.044
Observed data [$I > 2\sigma(I)$]	1736
$R_1[I > 2\sigma(I)]^a$	0.0474
wR_2 (all data)^b	0.1343
Goodness-of-fit on F^2	1.06
Completeness/%	97.4
Largest diff. peak and hole/(e·Å^{-3})	0.28 -0.15

a: $R_1 = \Sigma \{ |F_o| - |F_c| \} / \Sigma |F_o|$; b: $wR_2 = [\Sigma w(F_o^2 - F_c^2)^2 / \Sigma w(F_o^2)^2]^{1/2}$.

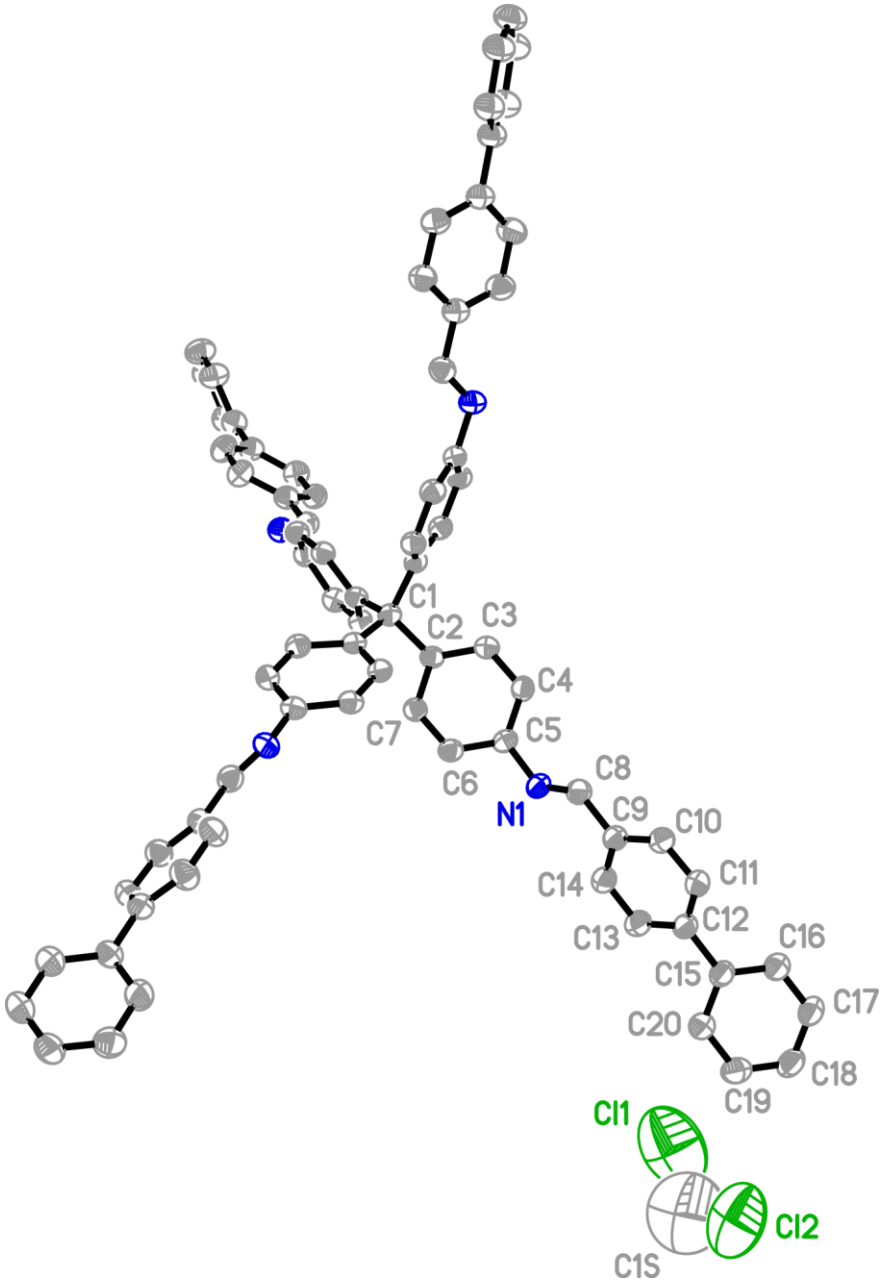

Figure S1. ORTEP drawing of the crystal structure of **E**. Thermal ellipsoids are displayed with 50% probability.

Section S2. *Fourier-transform infrared (FT-IR) spectroscopy analyses.*

The FT-IR spectra of starting materials, molecular analogue, and activated COFs were collected on a Bruker ALPHA FT-IR Spectrometer equipped with ALPHA's Platinum ATR single reflection diamond ATR module, which can collect IR spectra on neat samples. The signals are given in wavenumbers (cm^{-1}) and described as: very strong (vs), strong (s), medium (m), shoulder (sh), weak (w), very weak (vw) or broad (br).

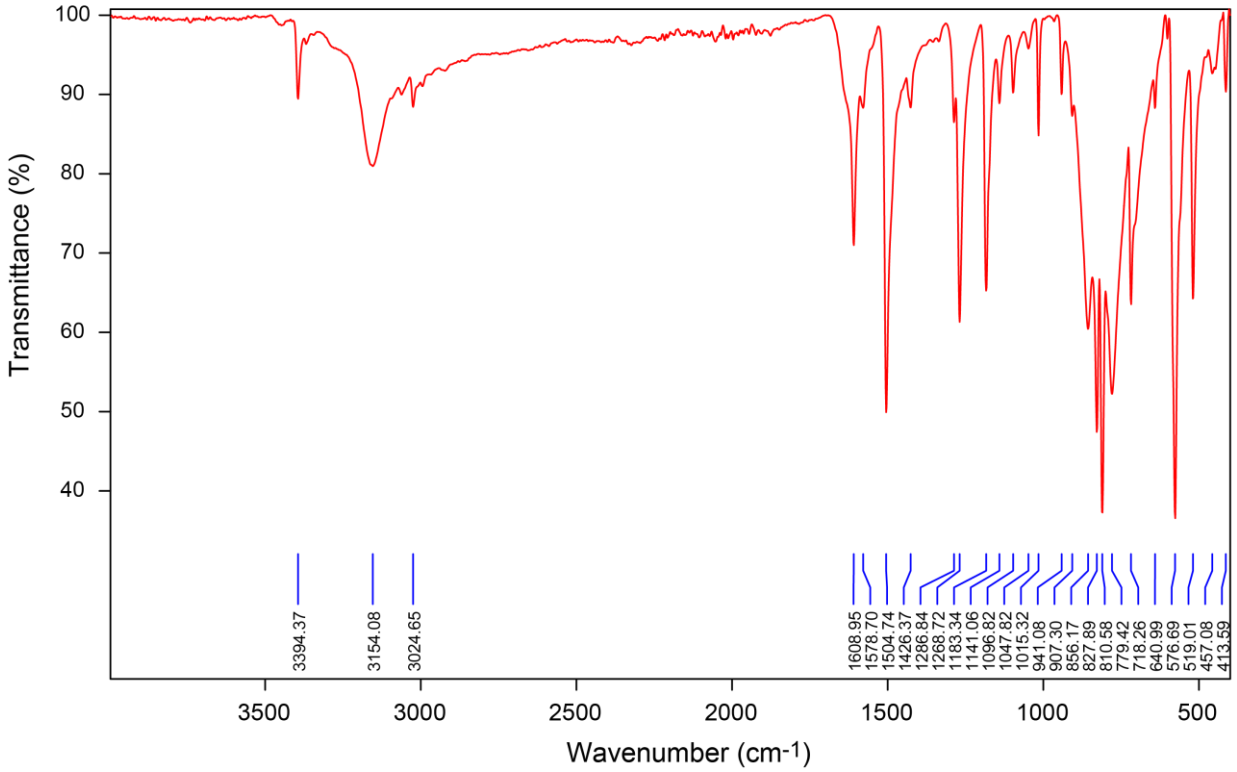

Figure S2. FT-IR spectrum of tetra-(4-anilyl)methane.

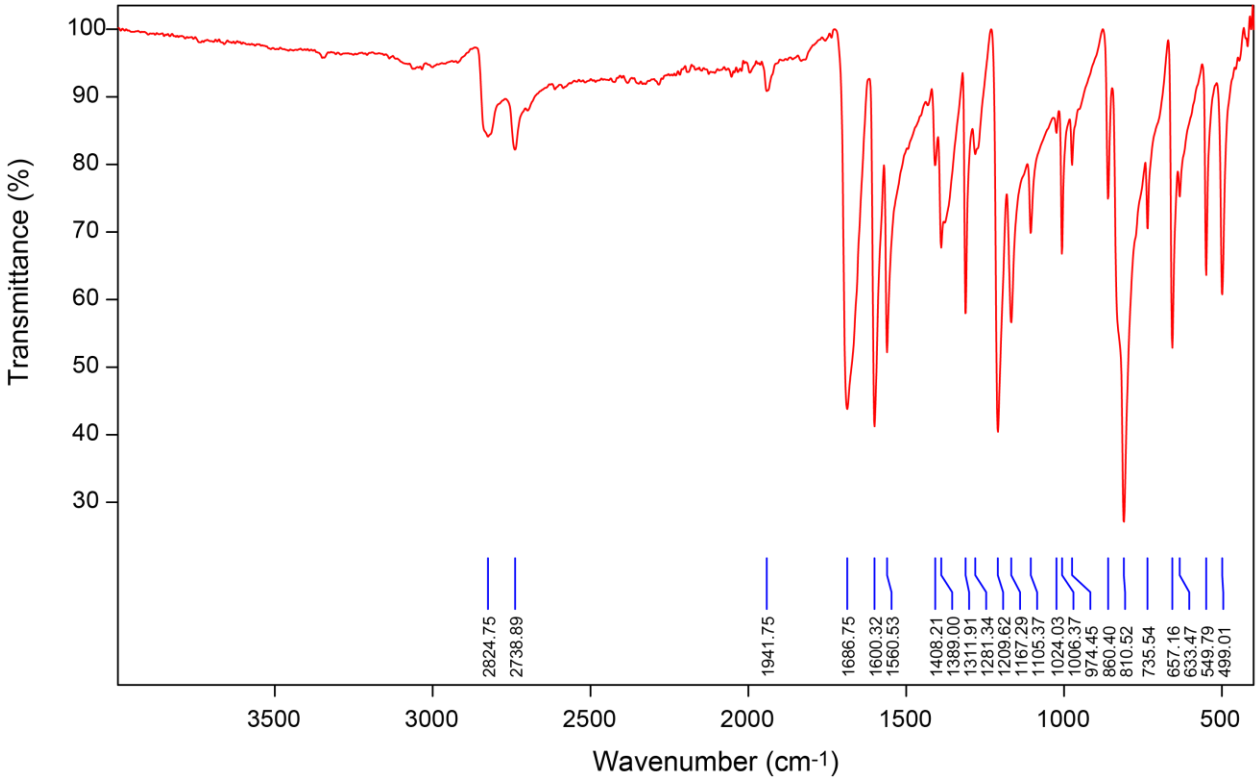

Figure S3. FT-IR spectrum of 4,4'-biphenyldicarbaldehyde.

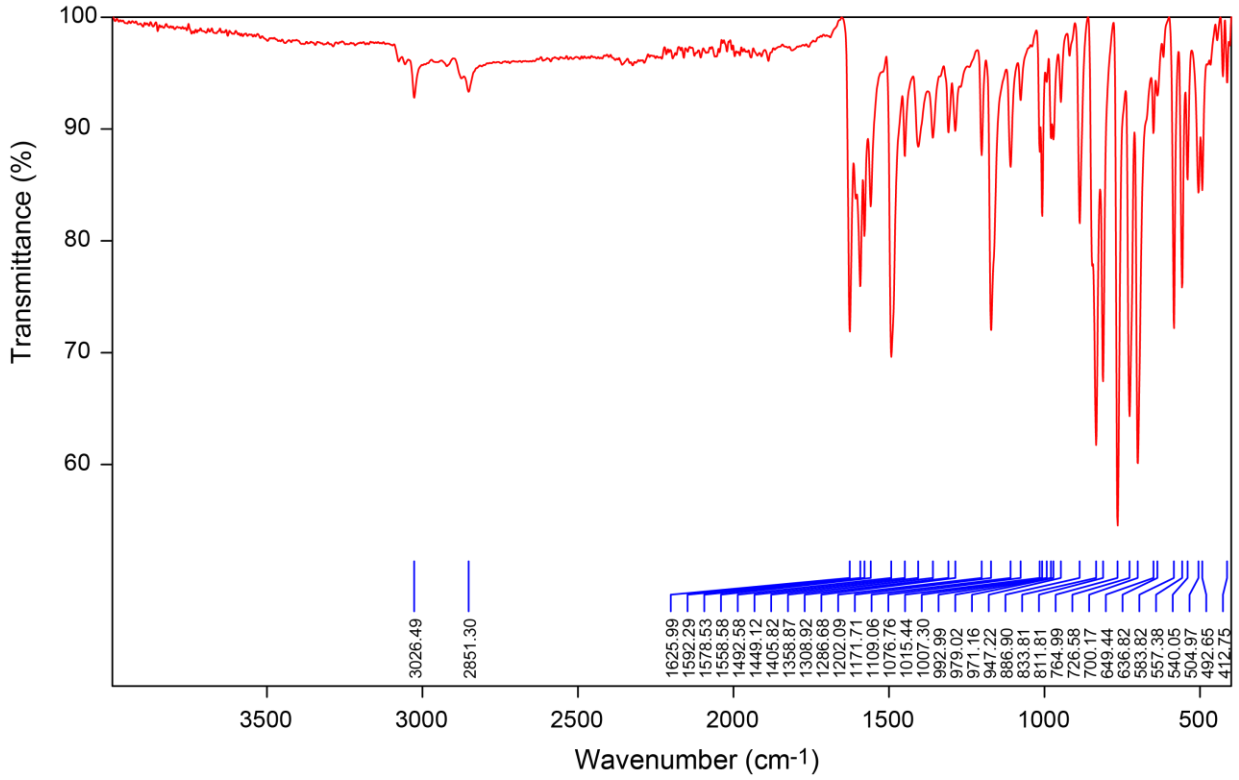

Figure S4. FT-IR spectrum of the molecular analogue for COF-320 (**E**).

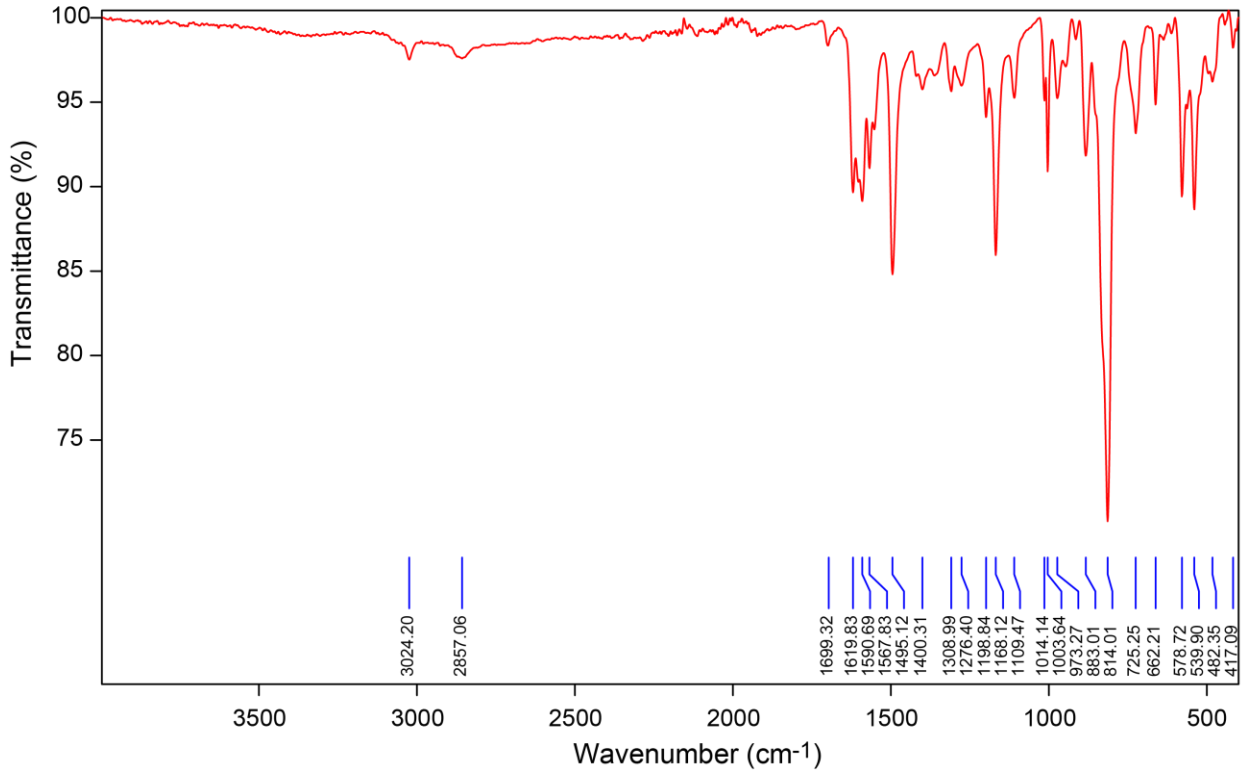

Figure S5. FT-IR spectrum of activated COF-320.

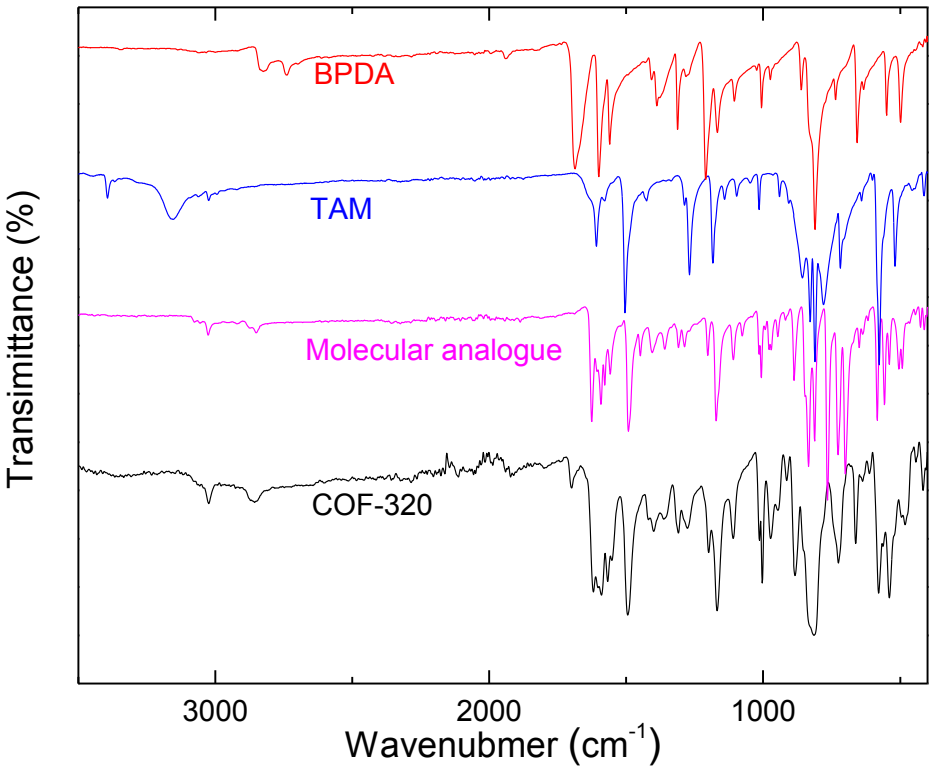

Figure S6. Stack plot of the FT-IR spectra for the comparison between starting materials, molecular analogue, and activated COF-320.

Table S2. Peak assignment for the FT-IR spectrum of COF-320. Notes and discussion are provided to correlate the spectra of starting material.

Peak (cm^{-1})	**Assignment and Notes**
3024.2 (w)	Aromatic C-H stretch from phenyl rings in tetraphenylmethane. Present in Model compound.
2875.1(vw)	Alkene C-H stretching from imine. Present in Model compound.
2857.1 (w)	Aromatic C-H stretch from phenyl rings in biphenyl. Present in Model compound.
1699.3 (w)	Aromatic C=C ring stretching from phenyl rings in tetraphenylmethane or biphenyl
1619.8 (m)	Imine C=N stretching. This bond is confirmed by the disappearance of the ν_{N-H} stretching mode from tetraanilylmethane (3394.4 cm^{-1} and 3154.1 cm^{-1}) and of the $\nu_{H-C=O}$ stretching mode from biphenyldicarboxaldehyde (2824.8 cm^{-1} and 2738.9 cm^{-1})
1607.1 (m)	Aromatic C=C ring stretching from phenyl rings in tetraphenylmethane.
1590.7 (m)	Aromatic C=C ring stretching from phenyl rings in biphenyl
1567.8 (m)	Aromatic C=C ring stretching from phenyl rings in biphenyl
1495.1 (s)	Aromatic C-C ring stretching from tetraphenylmethane
1420.6 (vw)	Aromatic C-C ring stretching from phenyl rings in tetraphenylmethane
1400.3 (w)	Aromatic C-C ring stretching from phenyl rings in biphenyl
1360.5 (vw)	Aromatic ring bending
1309.0 (w)	Aromatic ring stretching from biphenyl
1276.4 (w)	Aromatic ring stretching from tetraphenylmethane
1198.8 (w)	Imine C-C=N-C stretching. This mode is the stretching of the C-C and C-N single bonds
1168.1 (s)	C-Ph breathing. C-C stretching, characteristic of biphenyl
1110.2 (w)	C-Ph breathing. Tetrahedral C-C stretching, characteristic of tetraphenylmethane
1009.5 (w)	Aromatic C-H in plane bending from tetraphenylmethane
1003.6 (m)	Aromatic C-H in plane bending from biphenyl
973.3 (w)	Aromatic ring stretching from biphenyl
944.3 (w)	Aromatic ring stretching from tetraphenylmethane
914.9 (w)	Aromatic C-H phenyl ring substitution bands from tetraphenylmethane
883.0 (vw)	Aromatic C-H phenyl ring substitution bands from biphenyl
814.0 (vs)	Aromatic ring stretching from tetraphenylmethane
725.3 (m)	Aromatic ring stretching from tetraphenylmethane
662.2 (m)	C-Ph stretching, characteristic of biphenyl
637.5 (w)	C-Ph tetrahedral stretching, characteristic of tetraphenylmethane
578.7 (m)	Aromatic ring bending from tetraphenylmethane
539.9 (m)	Aromatic ring bending from biphenyl

Section S3. *Solid-state nuclear magnetic resonance (SSNMR) spectroscopy analyses.*

The solid-state nuclear magnetic resonance (SSNMR) spectra were collected on a Bruker AV-500 NMR spectrometer using a standard Bruker magic angle-spinning (MAS) probe with 4-mm (o.d.) zirconia rotors. The magic angle was adjusted by maximizing the number and amplitudes of the signals of the rotational echoes observed in the ^{79}Br MAS FID signal from KBr. The transmitter frequnce of ^{13}C NMR is 125.80 MHz, and that of ^{15}N NMR is 50.70 MHz.

The solid-state ^{13}C NMR spectra were acquired using cross-polarization (CP) MAS technique with the ninety degree pulse of ^{1}H with 4.2 μs pulse width. The CP contact time was 2 ms. High power two-pulse phase modulation (TPPM) ^{1}H decoupling was applied during data acquisition. The decoupling frequency corresponded to 32 kHz. The MAS sample spinning rates varied from 8 to 13.5 kHz. Recycle delays between scans were 2 s. The ^{13}C chemical shifts are given relative to neat tetramethylsilane as zero ppm, calibrated using the methylene carbon signal of adamantane assigned to 38.48 ppm as secondary reference.[2]

The solid-state ^{15}N CP/MAS NMR spectrum of the activated ^{15}N-enriched COF-320 was acquired using the ninety degree pulse for ^{1}H with 4.2 μs pulse width. The CP contact time was 5 ms. The MAS sample-spinning rate was 11 KHz. The decoupling frequency corresponded to 32 kHz. Recycle delays between scans was 10 s. The decoupling solid-state ^{15}N MAS NMR spectrum is more quantative to estmate the ratio of imine-^{15}N vs. redual amino-^{15}N, which was obtained using ninety degree pulse for ^{15}N with 4.0 μs pulse width. The recycle delay between scans was 25 s. The ^{15}N chemical shifts are given relative to liquid ammonia as zero ppm, calibrated using the nitrogen signal of α-glycine assigned to 32.4 ppm as secondary reference.[3]

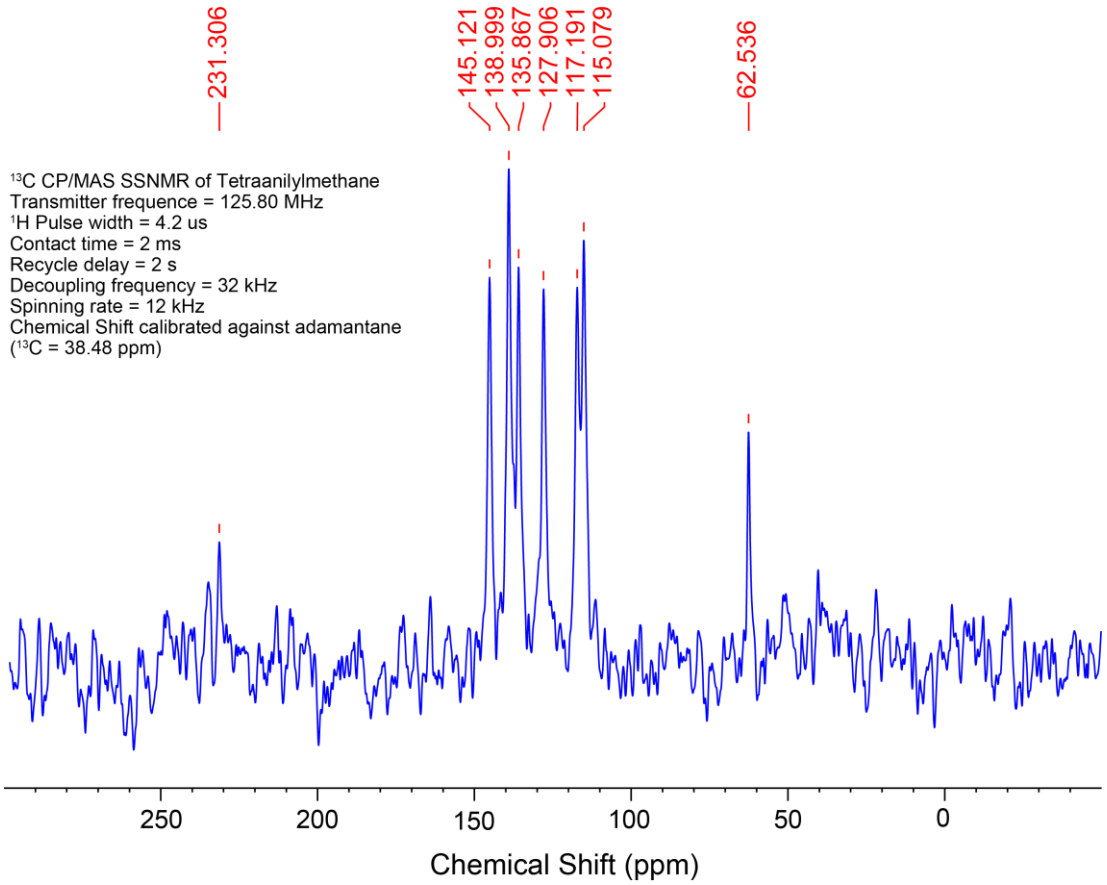

Figure S7. Solid-state ^{13}C CP/MAS NMR spectrum of tetra-(4-anilyl)-methane.

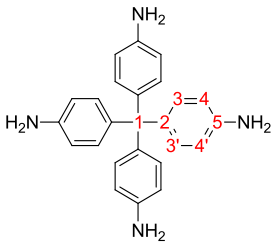

Chemical shift (ppm)	Assignment	Comments
62.626	1	Aliphatic quaternary carbon (alpha-aromataic, para-amino)
115.088 117.196	3, 3'	Aromatic carbon (beta-aliphatic, gamma-amino). In the solid state, this carbons are not related by symmetry.
127.888	2	Aromatic carbon (para-amino)
135.838 138.958	4, 4'	Aromatic carbon (gamma-aliphatic, beta-amino). In the solid state, this carbons are not related by symmetry.
145.061	5	Aromatic carbon (alpha-amino)
231.306	–	Spinning side band

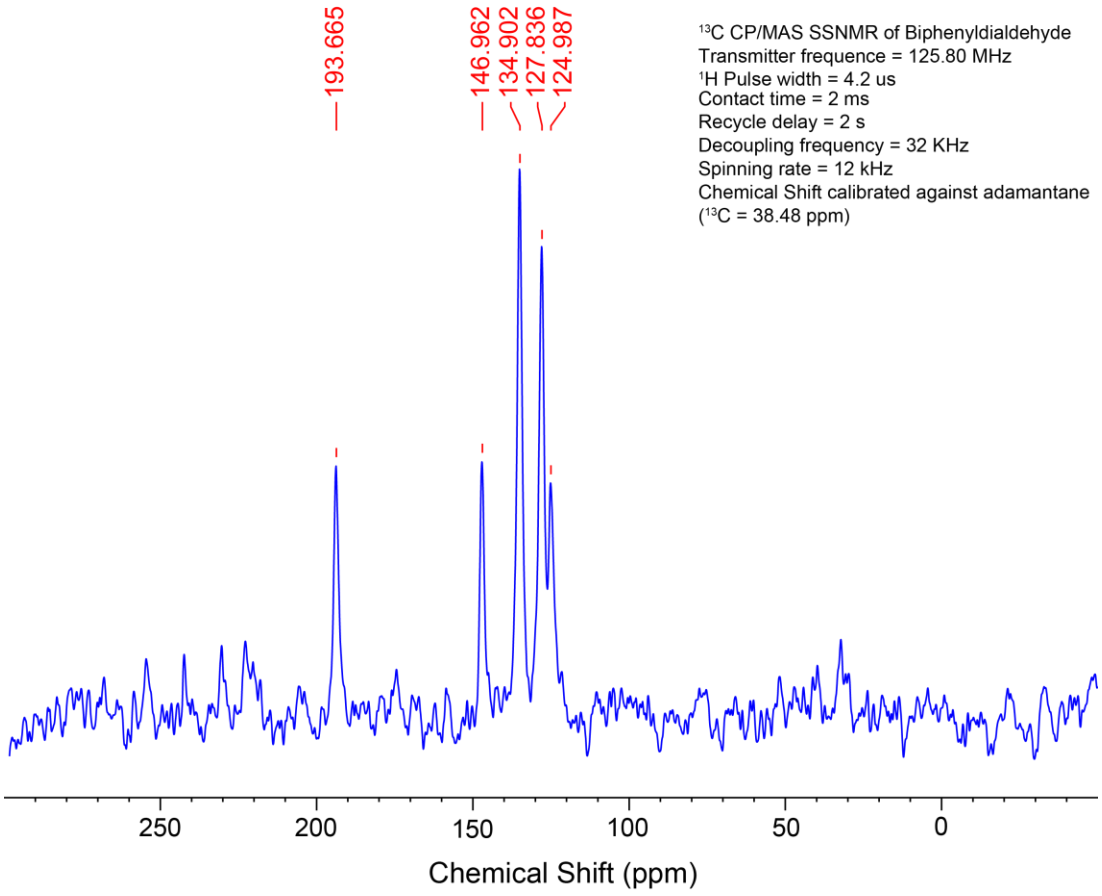

Figure S8. Solid-state ^{13}C CP/MAS NMR spectrum of 4,4'-biphenyldialdehyde.

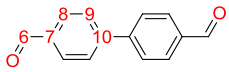

Chemical shift (ppm)	Assignment	Comments
124.987	9	Aromatic carbon (gamma-carbonyl)
127.836	8	Aromatic carbon (beta-carbonyl)
134.902	7	Aromatic carbon (alpha-carbonyl)
146.962	10	Aromatic carbon (para-carbonyl)
193.685	6	Carbonyl (alpha-aromatic)

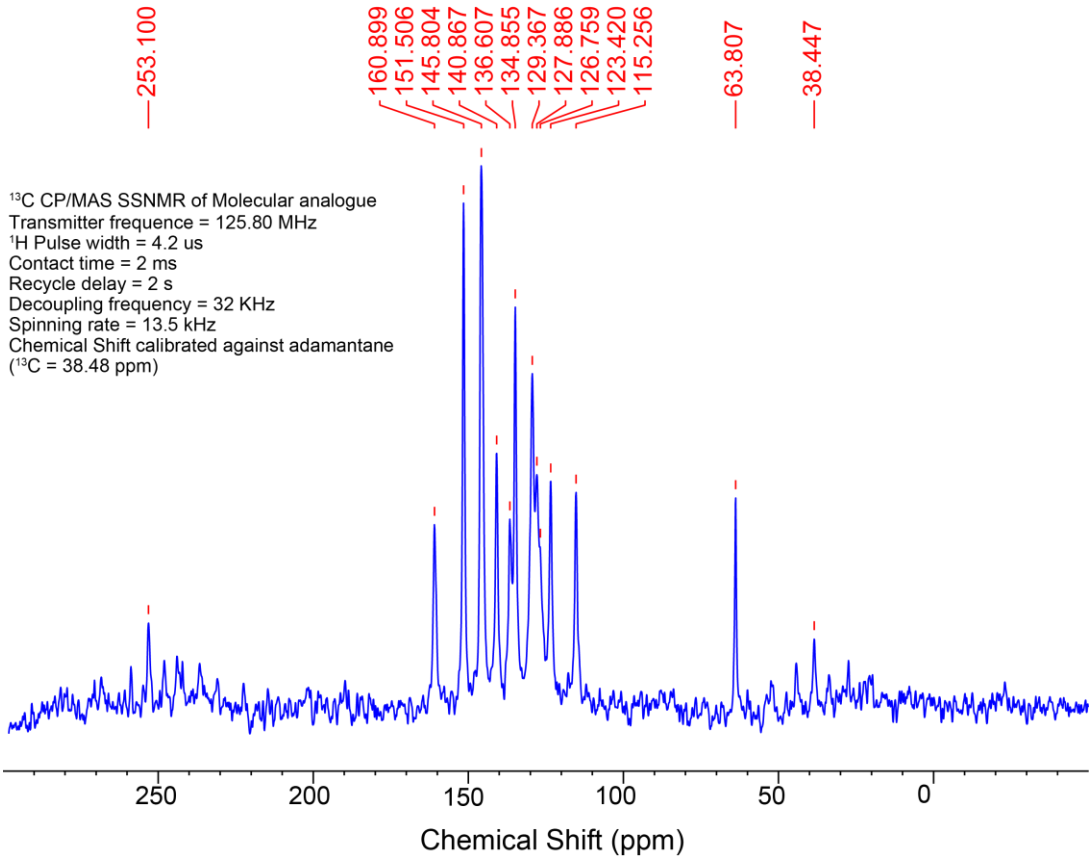

Figure S9. Solid-state ^{13}C CP/MAS NMR spectrum of molecular analogue.

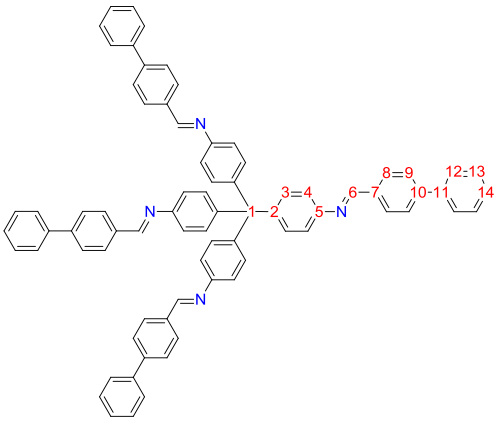

Signal (ppm)	Assignment	Comments
38.447	–	Spinning side band
63.807	1	Aliphatic quaternary carbon (alpha-aromatic)
115.256	3	Aromatic carbon (beta-aliphatic, gamma-imine)
123.420	9	Aromatic carbon (gamma-vinyl)
127.886	12	Aromatic carbon (beta-vinyl)
126.759	2	Aromatic carbon (alpha-aliphatic, para-imine)
129.367	8, 13	Aromatic carbon (beta-vinyl)
134.855	14	Aromatic carbon (para-aromatic)
136.607	7	Aromatic carbon (alpha-vinyl)
140.861	10, 11	Aromatic carbon (alpha-aromatic)
145.804	4	Aromatic carbon (beta-imine)
151.506	5	Aromatic carbon (alpha-imine)
160.899	6	Alkene carbon (alpha-imine, alpha-aromatic)
253.100	–	Spinning side band

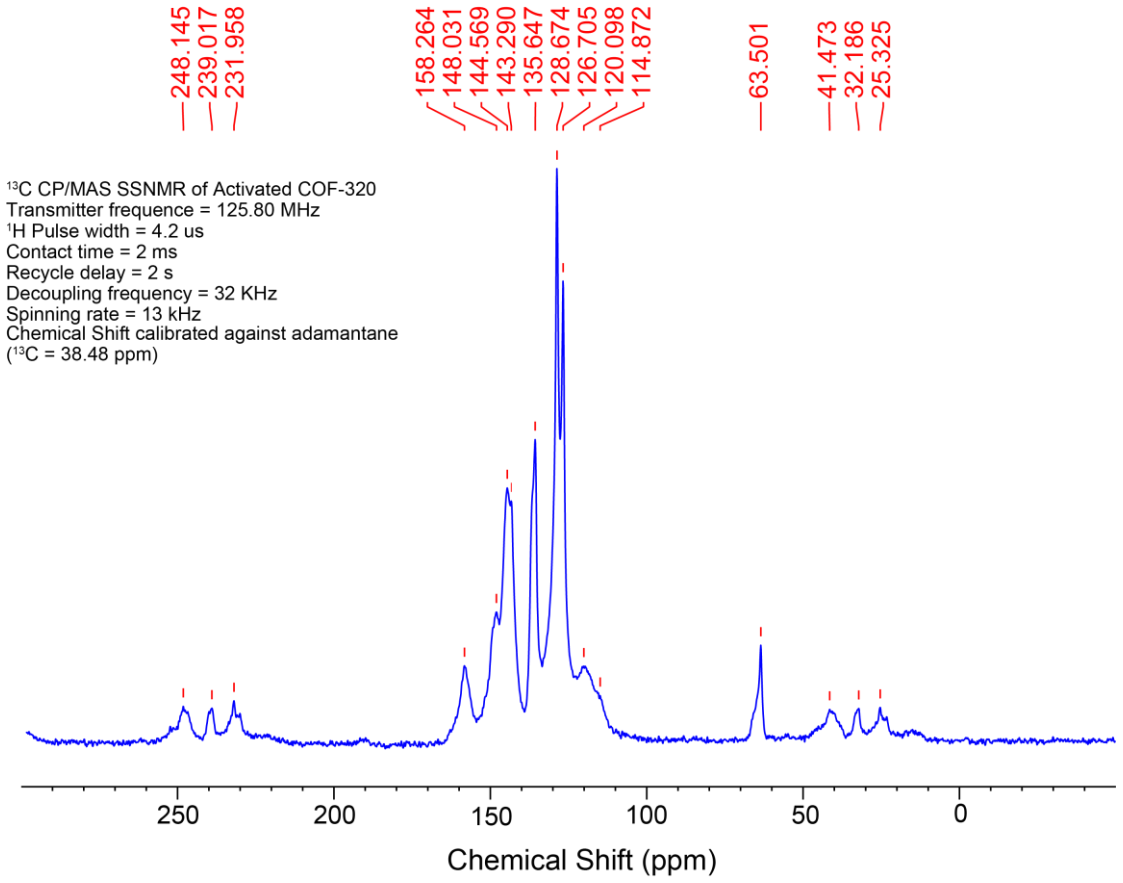

Figure S10. Solid-state ^{13}C CP/MAS NMR spectrum of activated COF-320

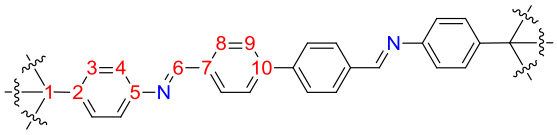

Chemical Shift (ppm)	Assignment	Comments
25.325	–	Spinning side band
32.186	–	Spinning side band
41.473	–	Spinning side band
63.480	1	Aliphatic quaternary carbon (alpha-aromatic)
114.862	3	Aromatic carbon (beta-aliphatic, gamma-imine)
120.088	9	Aromatic carbon (gamma-vinyl)
126.706	2	Aromatic carbon (alpha-aliphatic, para-imine)
128.677	8	Aromatic carbon (beta-vinyl)
135.663	7	Aromatic carbon (alpha-vinyl)
143.312	10	Aromatic carbon (alpha-aromatic)
144.603	4	Aromatic carbon (beta-imine)
148.051	5	Aromatic carbon (alpha-imine)
158.281	6	Alkene carbon (alpha-imine, alpha-aromatic)
231.958	–	Spinning side band
239.017	–	Spinning side band
248.145	–	Spinning side band

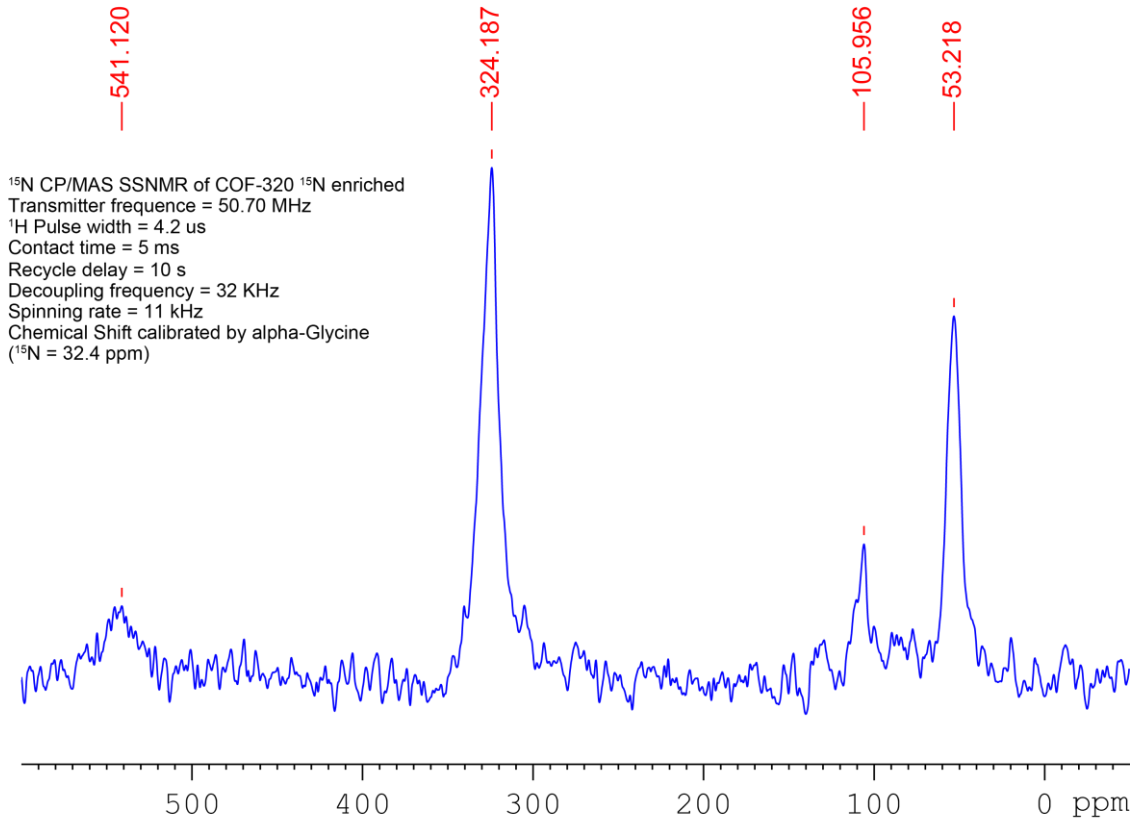

Figure S11. Solid-state ^{15}N CP/MAS NMR spectrum for activated ^{15}N-enriched COF-320.

Chemical Shift (ppm)	**Assignment**
53.218	Signal for residual aniline nitrogen from the terminal group on the surface of the crystallites and incompletely reacted group at defects in the materials and unreacted starting material
105.958	Spinning side band
324.187	Imine nitrogen
541.120	Spinning side band

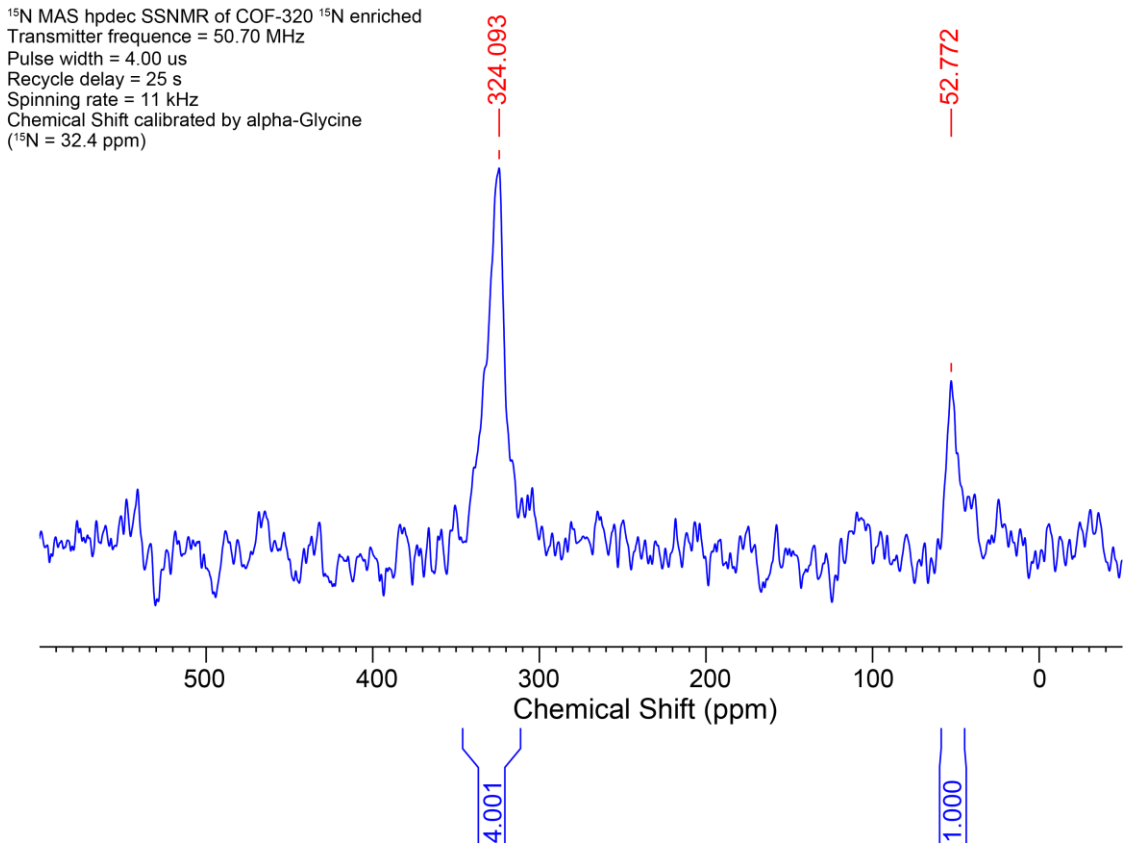

Figure S12. Solid-state ^{15}N high-power decoupling MAS NMR spectrum for activated ^{15}N-enriched COF-320.

Section S4. *Scanning electron microscopy (SEM) imaging.*

Samples of synthesized COF-320 were measured by dispersing the material onto a sticky carbon surface attached to a flat aluminum sample holder. Samples were analyzed on a JEOL JSM 6340F field-emission SEM operating at 3 kV. Only a homogenous morphology was apparent after exhaustive examination of a range of particle sizes that were deposited on the sample holder. Aggegration of oblong crystallites were observed (Figure S13) of size of 0.20 × 0.25 × 1.0 μm approximately. No evidence for the presence of other phases was observed in the surveyed samples.

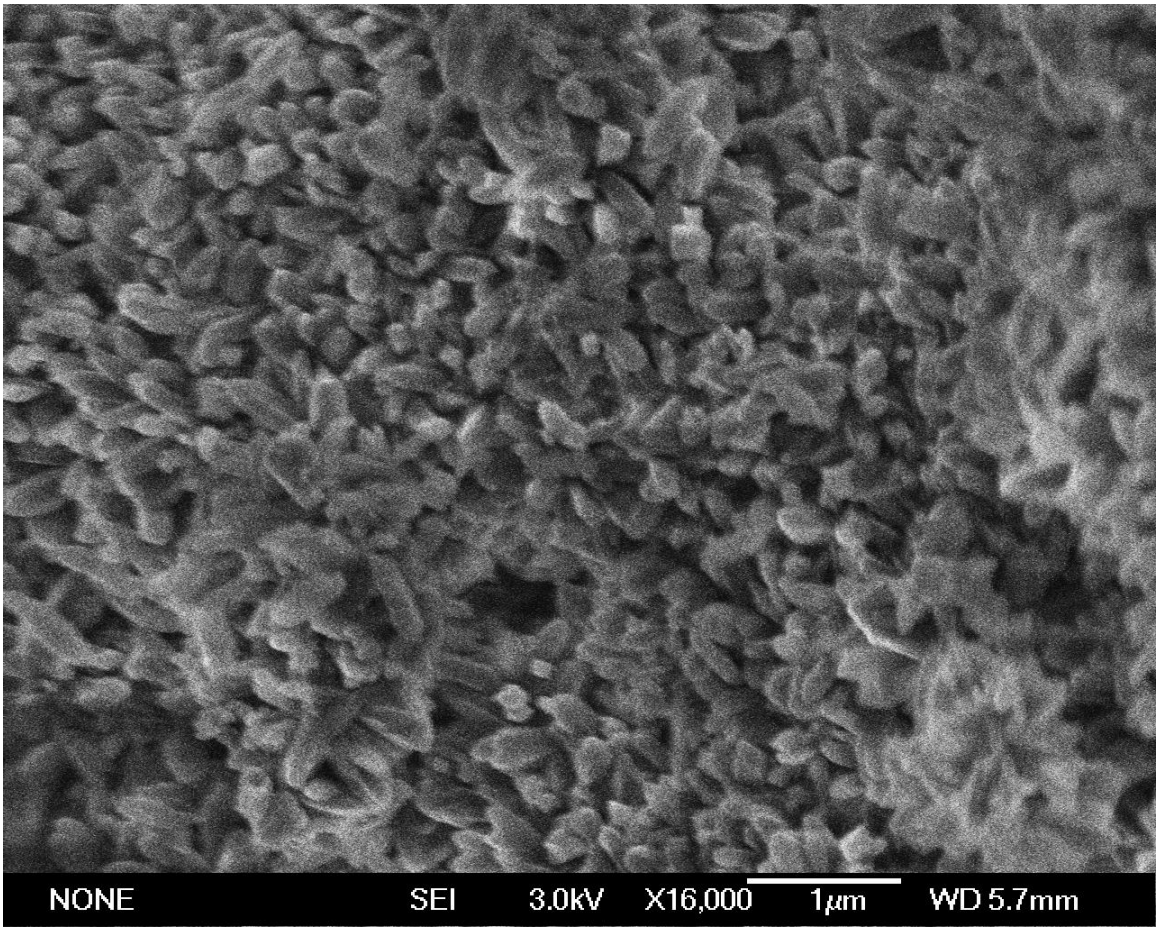

Figure S13. SEM image of COF-320 exhibiting aggregation of rice shaped crystals.

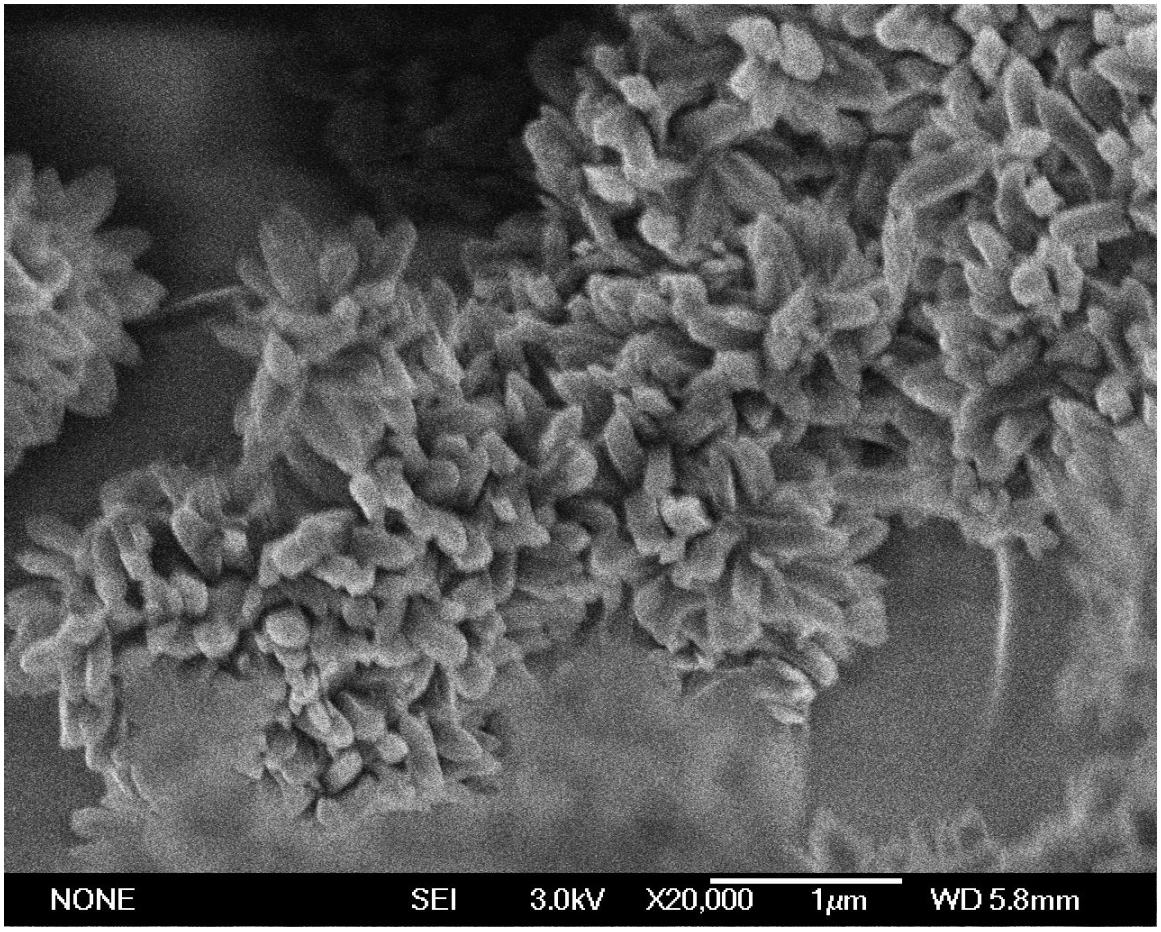

Figure S14. SEM image of COF-320 with high magnification.

Section S5. *Single-crystal structure determination by 3D rotation electron diffraction (RED).*

A COF-320 sample in THF was dispersed in tetrahydrofuran and treated by ultra-sonication for 4 minutes. A droplet of the suspension was transferred onto a carbon-coated copper grid. Three-dimensional (3D) rotation electron diffraction (RED) data of COF-320 was collected at 200 kV using the software *RED – data collection*[4] on a JEOL JEM2100 TEM. The RED data was collected in selected-area electron diffraction (SAED) mode. During the RED data collection, the electron beam was fully spread over the whole phosphorus screen. The selected-area aperture used for RED data collection was about 1.6 μm in diameter, which is much larger than the maximum crystal size of COF-320 (< 1 μm). We tracked the crystal in image mode to ensure that the entire crystal was inside the aperture throughout the data collection. In total, 396 ED frames were recorded at 89 K using a cryogenic sample holder. The crystal tilt range was from -34.19º to 38.33º with the tilt step of 0.20º. Each ED frame was recorded under the spot size 2 with the exposure time 1s. The total data collection time was 21 min. For the data collected at 298 K, 150 ED frames were recorded. The crystal tilt range was from -35.00º to 25.10º with the tilt step of 0.40º, and each ED frame was recorded under the spot size 3 with the exposure time 3s. The data processing was conducted using the software *RED – data processing*,[4] including peak search, unit cell determination, indexation of reflections and intensity extraction.

The structure of COF-320 was solved against the intensities obtained from the 3D-RED data collected at 89 K using the simulated annealing parallel tempering algorithm implemented in the program *FOX*.[5] Final structure refinement was done using the SHELXL-97 program.[6] Due to the large pore sizes and possible disorders of the guest THF molecules in the pores, it was not possible to locate the guest molecules in the channels. The PLATON/SQUEEZE program[7] was used to remove the scattering contribution from the disordered guest molecules and to produce solvent-free diffraction intensities, which were used in the final structure refinement. Crystallographic data and details of structure refinement are presented in Table S3.

Table S3. The RED data collection and structure determination details of COF-320.

Chemical Formula	$C_{53}H_{36}N_4$
Formula weight	728.86
Temperature (K)	89
Wavelength (Å)	0.0251
Crystal system	Tetragonal
Space group	*I*-42*d* (*No*.122)
a (Å)	30.17
c (Å)	7.28
V (Å^3)	6628
Z	4
$d_{calc.}$ (g cm^{-3})	0.730
F(000)	630
Crystal size (μm)	1.0×0.5×0.2
Crystal color	yellow
Tilt range	-34.19° ~ +38.33°
Tilt step	0.2°
No. of frames	396
Resolution (Å)	1.5
Completeness	0.975
Reflections collected	3424
Unique reflections	570
R_{int}	0.481
Final *R* indices[$I > 2\sigma(I)$]	$R_1 = 0.3100$, $wR_2 = 0.6386$
R indices (all data)	$R_1 = 0.3821$, $wR_2 = 0.6677$
No. of parameters	21
No. of restraints	31

Table S4. Fractional atomic coordinates for crystal structure of COF-320 at 89 K.

COF-320 at 89 K			
Space group: *I*-42*d* (*No*.122) $a = b = 30.17$ Å; $c = 7.28$ Å $\alpha = \beta = \gamma = 90°$ $V = 6628$ Å^3 $Z = 4$			
Atom	*x*	*y*	*z*
C1	0	0	0
C2	-0.0113	0.0386	0.1281
C3	-0.0494	0.0351	0.2340
H3	-0.0673	0.0102	0.2243
C4	-0.0607	0.0689	0.3550
H4	-0.0862	0.0666	0.4264
C5	-0.0338	0.1062	0.3700
C6	0.0043	0.1097	0.2640
H6	0.0223	0.1346	0.2739
C7	0.0156	0.0759	0.1430
H7	0.0411	0.0782	0.0718
N8	-0.0432	0.1392	0.5060
C9	-0.0684	0.1350	0.6480
H9	-0.0840	0.1085	0.6612
C10	-0.0743	0.1682	0.7880

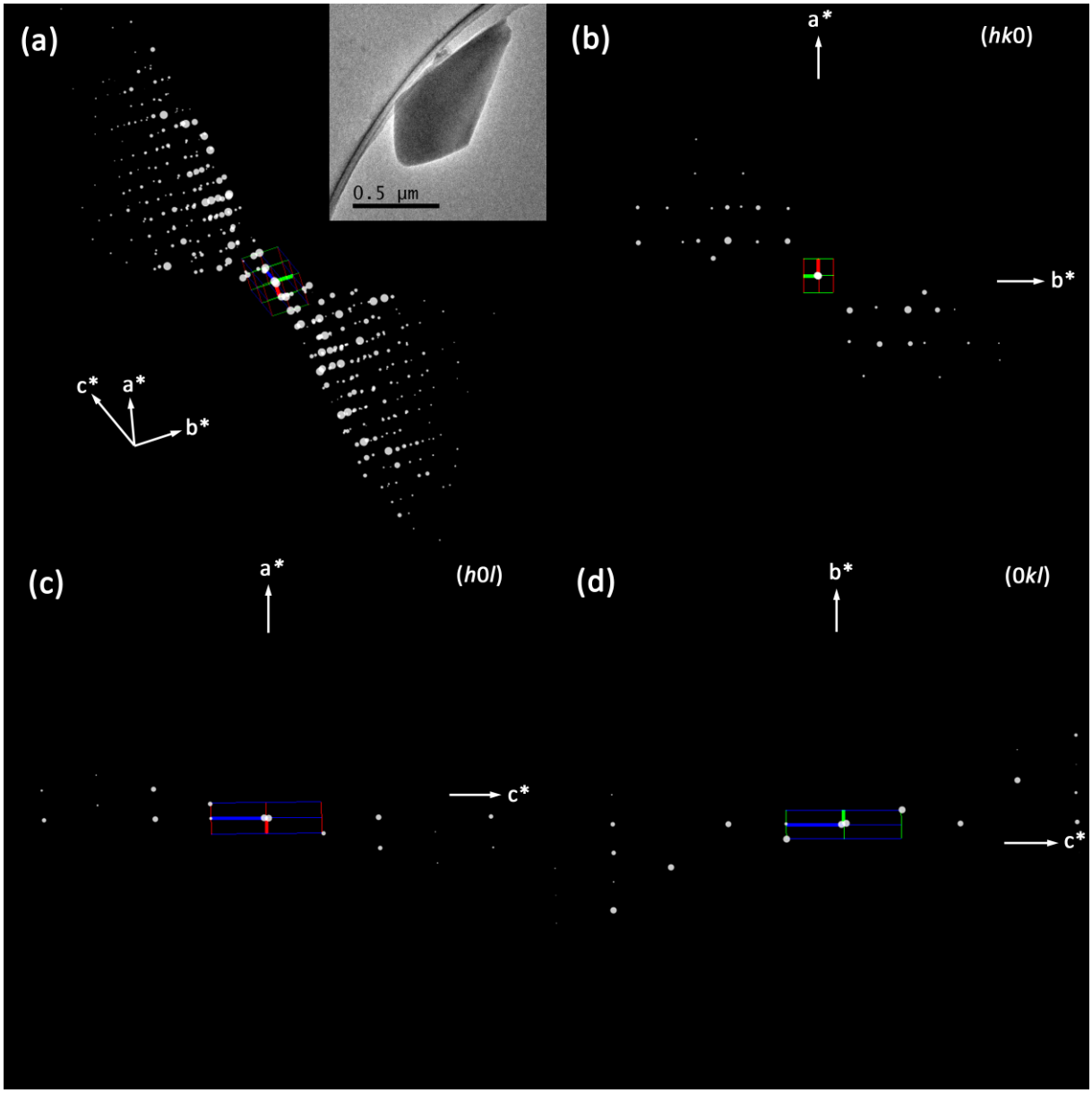

Figure S15. Reconstructed reciprocal lattice of COF-320 from 3D-RED data at 298 K (a). 2D slices (b-d) of the reconstructed reciprocal lattice obtained from the 3D RED data.

Section S6. *Crystal structure modeling and powder X-ray diffraction (PXRD) analyses.*

Crystal structure modeling. The room temperature crystal structure of COF-320 was built based on the unit cell and space group symmetry determined from RED data on COF-320 crystals at 298 K using *Materials Studio 5.0* to generate the 3D atomistic file. The crystal structure was constructed from the atoms of the central C atoms of the tetrahedral units whose coordinates were solved from the RED data, and was geometrically optimized with the *Forcite* module using the *Universal* force field after defining all the types of bonds.

Table S5. Fractional atomic coordinates for crystal structure model of COF-320 at 298 K.

COF-320 at 298 K			
Space group: *Imma* (No. 74) a = 27.93 Å; b = 31.31 Å; c = 7.89 Å $\alpha = \beta = \gamma = 90°$ V = 6899 Å^3 $Z = 2$			
Atom	*x*	*y*	*z*
C1	0.5433	0.3058	0.3960
C2	0.5433	0.3409	0.2867
C3	0.4375	0.2114	0.7689
C4	0.4000	0.2114	0.8861
H5	0.5773	0.2923	0.4322
H6	0.5769	0.3537	0.2412
H7	0.4516	0.1810	0.7285
H8	0.3863	0.1814	0.9338
C9	0.5431	0.4361	-0.2338
C10	0.5433	0.4671	-0.3615
C11	0.3094	0.2115	1.4482
C12	0.2804	0.2114	1.5928
H13	0.5769	0.4238	-0.1865
H14	0.5780	0.4772	-0.4046
H15	0.3212	0.1815	1.3948
H16	0.2710	0.1804	1.6415
C17	0.5000	0.2500	0.5818
C18	0.5000	0.2889	0.4603
C19	0.5000	0.3590	0.2340
N20	0.5000	0.3936	0.1160
C21	0.5000	0.4834	-0.4298
C22	0.5000	0.4207	-0.1692
C23	0.5000	0.3859	-0.0452
H24	0.5000	0.3534	-0.0900
C25	0.4563	0.2500	0.7036
C26	0.3811	0.2500	0.9448
N27	0.3449	0.2500	1.0727
C28	0.2653	0.2500	1.6704
C29	0.3239	0.2500	1.3755
C30	0.3585	0.2500	1.2364

Powder X-ray diffraction data collection. Powder X-ray diffraction data were collected using a Bruker D8-advance θ-θ diffractometer in parallel beam geometry employing Cu Kα line focused radiation at 1600 W (40 kV, 40 mA) power and equipped with a position sensitive detector with at 6.0 mm radiation entrance slit. Samples were mounted on zero background sample holders by dropping powders from a wide-blade spatula and then leveling the sample with a razor blade. For the THF exchanged sample, an air-tight sample holder was employed to avoid solvent evaporation during the data acquisition. The best counting statistics were achieved by collecting samples using a 0.02º 2θ step scan from 1 – 50º with exposure time of 5 s per step. The Pawley PXRD refinement is performed using the Reflex module in the Materials Studio 5.0, in which a Pseudo-Voigt profile function was used for the profile fitting (peak broadening, peak asymmetry, and zero shift error were taken into account). Unit cell and sample parameter were refine at the meantime.

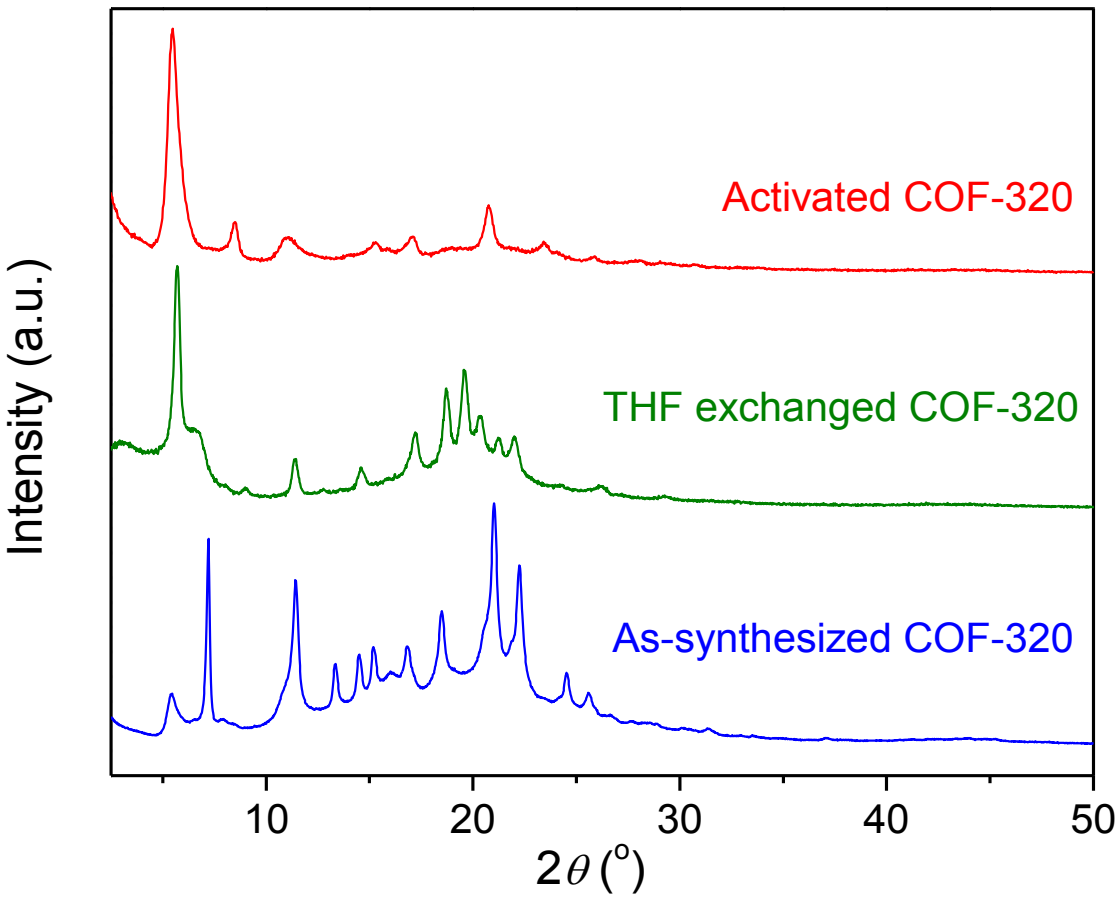

Figure S16. PXRD patterns of as-synthesized, THF-exchanged, and supercritical CO_2 activated samples of COF-320.

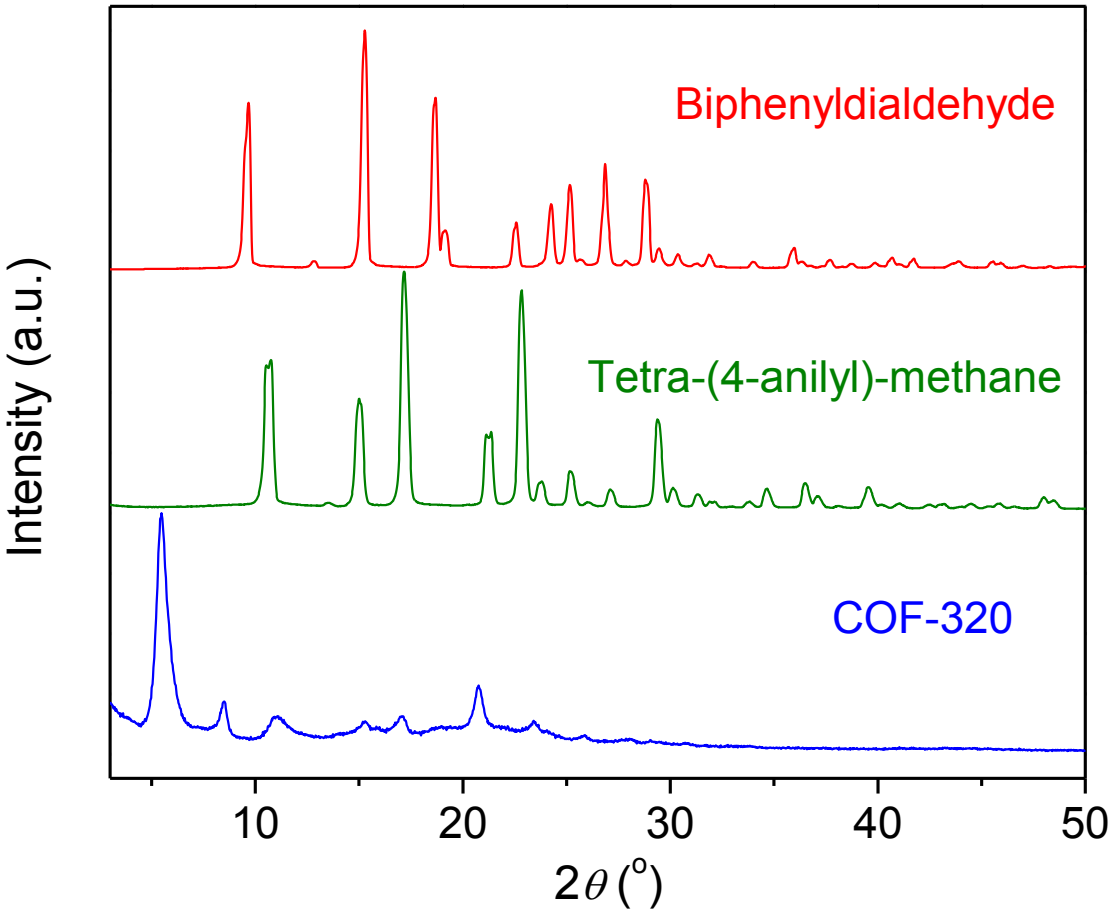

Figure S17. PXRD patterns of COF-320, biphenyldialdehyde, and tetra-(4-anilyl)-methane.

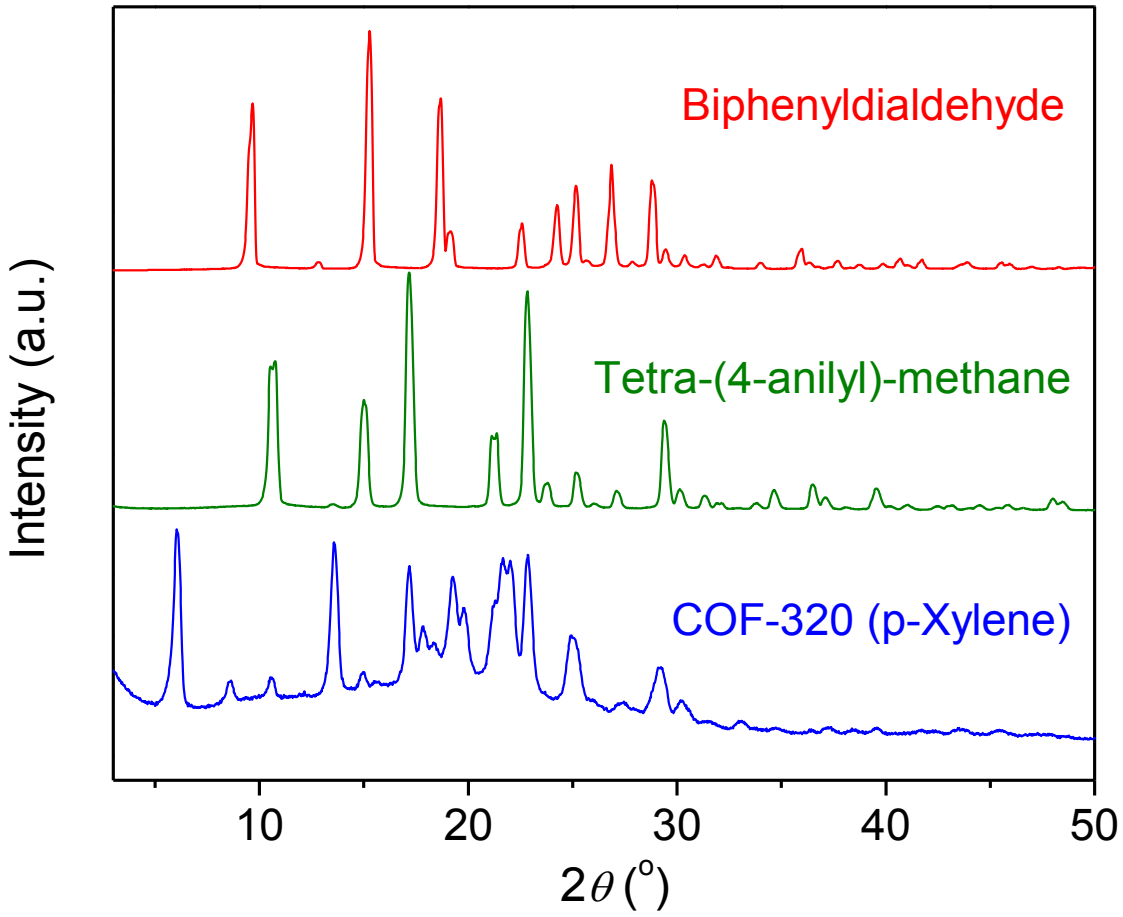

Figure S18. PXRD pattern of COF-320 synthesized from p-Xylene and comparison with the patterns of the starting materials. (Similar reaction was performed by replacing dioxane into p-Xylene without adding acetic acid, and the product was washed with dioxane and THF. The imine-bond formation was also confirmed by IR with the imine stretching vibrations at 1619 and 1202 cm^{-1}. However, the yield (< 20 %) is much lower than that of dioxane protocol, and starting materials was removed by washing using dioxane.)

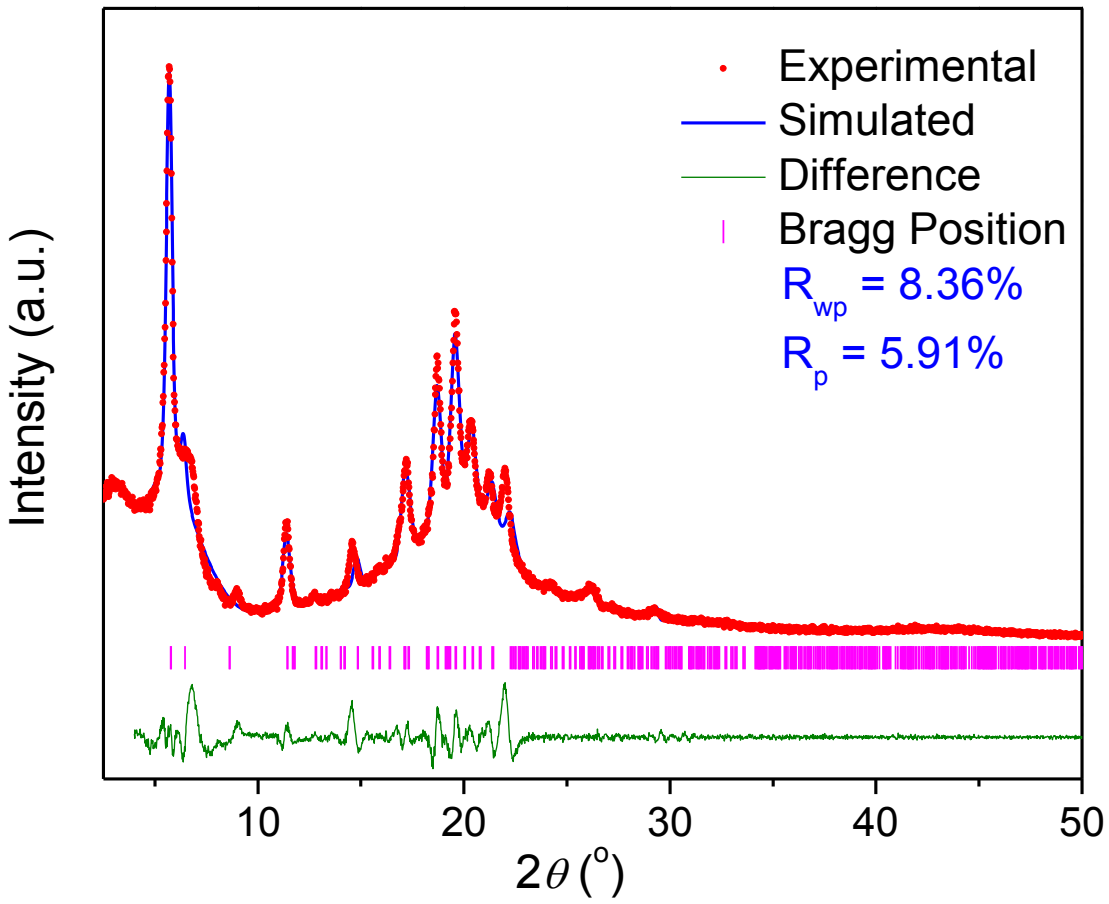

Figure S19. PXRD full pattern profile refinement of THF-exchanged COF-320 (unit cell after refinement: a = 27.88(0.03) Å, b = 31.28(0.04) Å, c = 7.882(0.008) Å, V = 6874 (13) Å^3).

Section S7. *Thermogravimetric analysis (TGA).*

Samples were run on a TA Instruments Q-500 series thermal gravimetric analyzer with samples held in a platinum pan under nitrogen atmosphere. A ramp rate of 5 °C/ min was used.

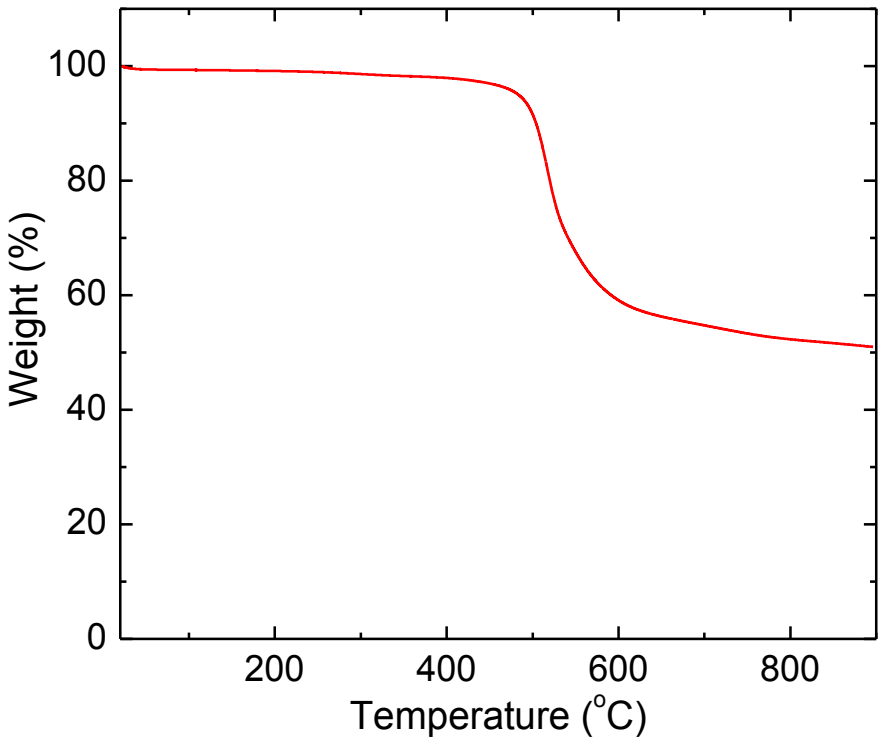

Figure S20. TGA trace for activated COF-320.

Section S8. *Low pressure (0 – 110 kPa) methane sorption measurements.*

Low-pressure (0 – 110 kPa) gas sorption isotherms were measured volumetrically using a Quantachrome Autosorb-1 automated adsorption analyzer. Gas sorption measurements at 273, 283, and 298 K were taken with a water bath whose temperatures were controlled by a recirculating chiller. The used gases (He, Ar, N_2, and CH_4) were UHP grade. The adsorption affinities were estimated from isotherms at different temperatures applying the Virial fitting method.[8]

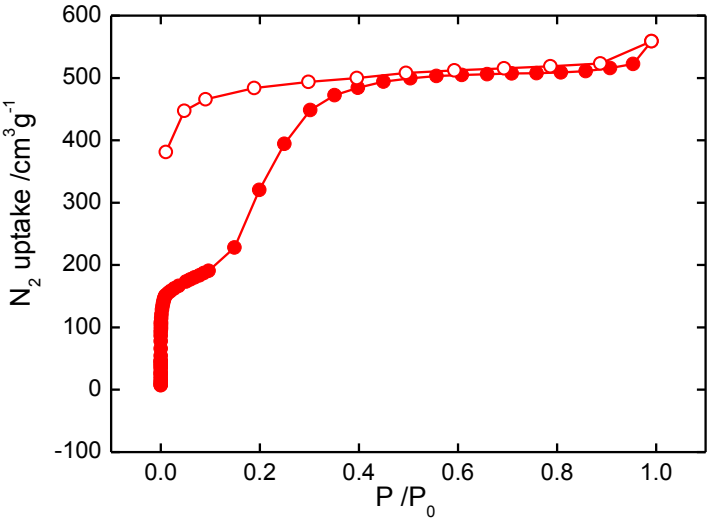

Figure S21. N_2 adsorption isotherm of COF-320 at 77 K.

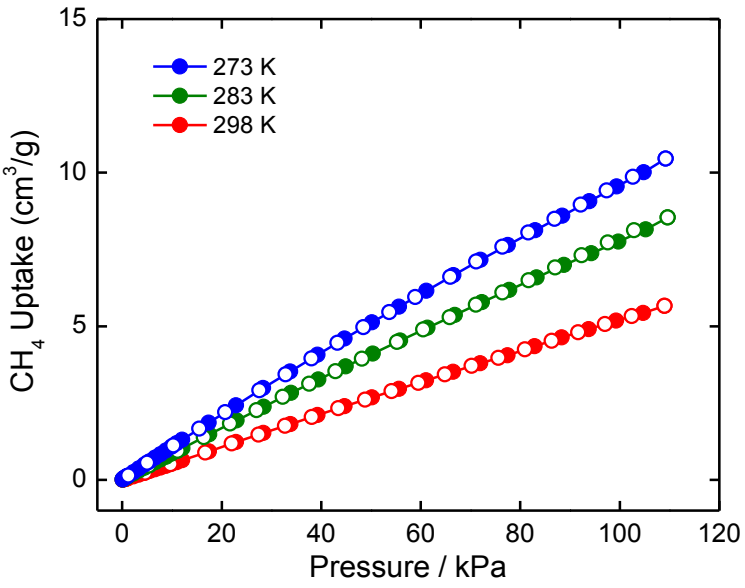

Figure S22. Low-pressure methane adsorption isotherms for COF-320 at 273, 283, and 298 K, respectively.

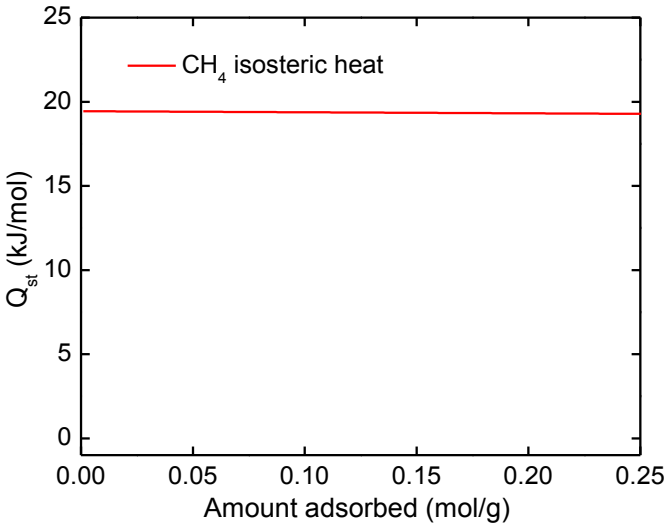

Figure S23. Coverage-dependent isosteric heat of methane for COF-320.

Section S9. *High pressure (0 – 80 bar) methane sorption measurements.*

High-pressure (0 – 80 bar) gas adsorption isotherms were measured volumetrically using a HPVA-100 high-pressure adsorption analyzer (VTI Corp.). The temperature was controlled by the water bath with a recirculating chiller. The gravimetric methane total uptake is calculated taking both the mass of COF and the mass of adsorbed methane into account of the denominator.[9]

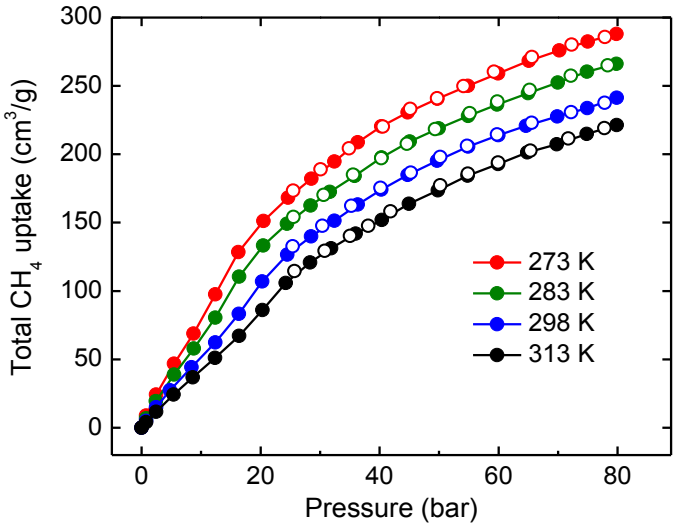

Figure S24. High-pressure methane total uptake for COF-320 at 273, 283, 298, and 313 K, respectively.

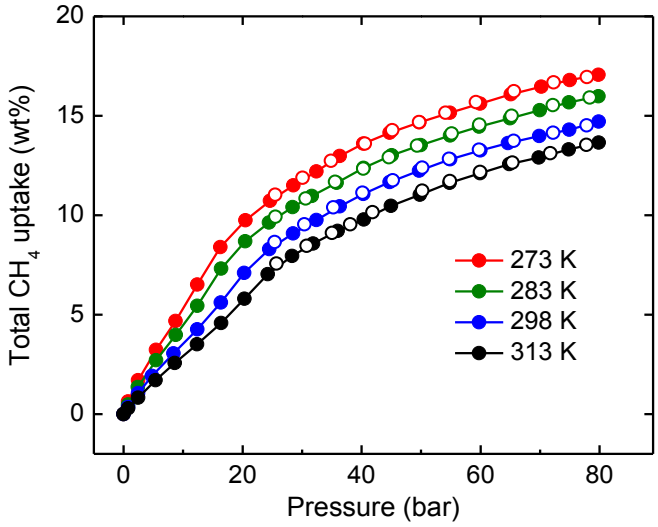

Figure S25. Gravimetric methane total uptake for COF-320 at 273, 283, 298, and 313 K, respectively.

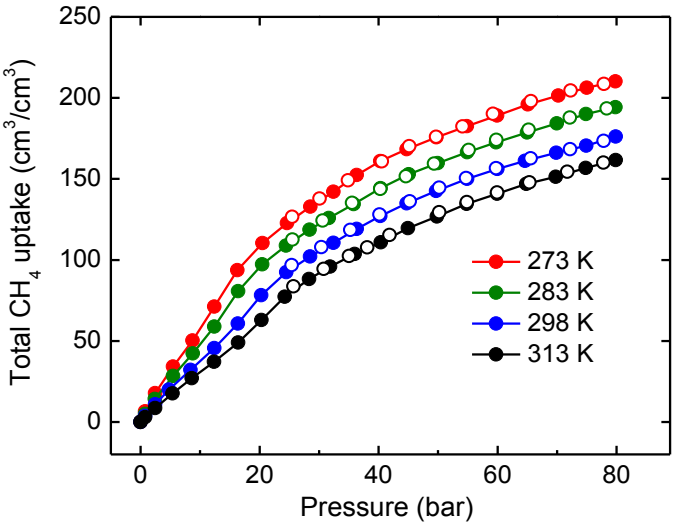

Figure S26. Volumetric methane total uptake for COF-320 at 273, 283, 298, and 313 K, respectively.

References:

(1) Plietzsch, O.; Schilling, C. I.; Tolev, M.; Nieger, M.; Richert, C.; Muller, T.; Brase, S. *Org. Biomol. Chem*. **2009**, *7*, 4734.

(2) Morcombe, C. R.; Zilm, K. W. *J. Magn. Reson.* **2003**, *162*, 479.

(3) Taylor, R. E.; Dybowski, C. *J. Mol. Struct.* **2008**, *889*, 376.

(4) Wan, W.; Sun, J. L.; Su, J.; Hovmöller, S.; Zou, X. *J. Appl. Crystallogr.* **2013,** accepted.

(5) Favre-Nicolin, V.; Černý, R. *J. Appl. Crystallogr.* **2002**, *35*, 734.

(6) Sheldrick, G. *Acta Crystallgr. A* **2008**, *64*, 112.

(7) Spek, A. *Acta Crystallgr. D* **2009**, *65*, 148.

(8) Czepirski, L.; Jagiełło, J. *Chem. Eng. Sci.* **1989**, *44*, 797.

(9) T. A. Makal, J.-R. Li, W. Lu, H.-C. Zhou. *Chem. Soc. Rev.*, **2012**, *41*, 7761.